Detection of Multiple Movers Based on Single Channel Source Separation of Their Micro-Dopplers

SHELLY VISHWAKARMA, Student Member, IEEE
SHOBHA SUNDAR RAM, Member, IEEE
Indraprastha Institute of Information Technology Delhi, New Delhi, India

Studies have demonstrated the usefulness of micro-Doppler signatures for classifying dynamic radar targets such as humans, helicopters, and wind turbines. However, these classification works are based on the assumption that the propagation channel consists of only a single moving target. When multiple targets move simultaneously in the channel, the micro-Dopplers, in their radar backscatter, superimpose thereby distorting the signatures. In this paper, we propose a method to detect multiple targets that move simultaneously in the propagation channel. We first model the micro-Doppler radar signatures of different movers using dictionary learning techniques. Then, we use a sparse coding algorithm to separate the aggregate radar backscatter signal from multiple targets into their individual components. We demonstrate that the disaggregated signals are useful for accurately detecting multiple targets.

Manuscript received August 22, 2016; revised March 15, 2017 and July 18, 2017; released for publication July 25, 2017. Date of publication August 15, 2017; date of current version February 7, 2018.

DOI. No. 10.1109/TAES.2017.2739958

Refereeing of this contribution was handled by P. Lombardo.

This work was supported in part by the Department of Science and Technology, Government of India, in part by DST Inspire fellowship, and in part by the Air Force Office of Scientific Research, AOARD under Grantt 5IOA036 FA23861610004.

Authors addresses: S. Vishwakarma and S. S. Ram are with Indraprastha Institute of Information Technology Delhi, New Delhi 110020, India E-mails: (shellyv@iiitd.ac.in; Shobha@iiitd.ac.in). *(Corresponding author: Shelly Vishwakarma.)*

0018-9251 © 2017 IEEE

I. INTRODUCTION

Targets that undergo micromotions such as rotation and vibration along with the bulk body translational motion give rise to frequency modulations along the main Doppler called micro-Dopplers [1], [2]. Extensive studies over the last decade have demonstrated that micro-Doppler features can be exploited for the classification of a variety of ground moving targets such as vehicles, animals [3]–[6], wind turbines [7], and airborne targets [8]–[10]. However, a majority of the works in this area have focused on using micro-Dopplers for identifying different human activities [11]–[39]. Radar detection of humans may be of particular interest for law enforcement, security, and biomedical applications. Humans are rarely still and the movements of their arms and legs give rise to micro-Dopplers [11]. As a result, Doppler sensors have been used to detect both periodic motions, such as the human gait [11], [13]–[18], and nonperiodic motions of the arms or legs [19], [20]. Fioranelli *et al.* [21], [22] investigated the possibility of distinguishing between armed and unarmed personnel based on their micro-Doppler signatures. The backscattered data from dynamic targets have mostly been gathered by narrow-band Doppler radars at microwave frequencies. Alternatively, wideband radar [23], [24], millimeter radar [20], [25], and acoustic sensors [11], [26] have also been deployed for gathering micro-Doppler data. Subsequently, discriminative features have been extracted from time-frequency representations of the micro-Doppler data. The algorithms have ranged from heuristic techniques [13], [39], to more sophisticated methods based on principle component analysis [30], [31], independent component analysis [32], empirical mode decomposition [20], and Hilbert–Huang transform [32], [34]. Studies have also been carried out to determine the most informative features in the micro-Doppler signatures for classification [37]. Once the features are extracted, algorithms such as support vector machine [13], [20], [23] and Bayesian classifier [4], [38] have been used for classification purposes. More recently, Kim and Moon [39] used deep convolution neural networks, which jointly learnt informative features and classification boundaries without using an additional feature extraction algorithm.

All of these works are based on the underlying assumption that the channel consists of only a single dynamic target or target class during detection. When multiple targets are present simultaneously in the channel, their radar backscatter superimpose. As a result, the signatures are dominated by features arising from the strongest targets (based on their radar cross section and proximity to the radar) with distortions arising from the weaker target returns. The distorted micro-Doppler signatures are then incorrectly classified. This is a serious limitation in most real world scenarios since they often consist of multiple movers. For instance, indoor environments may consist of moving humans, fans, and loudspeakers, while outdoor environments may comprise humans, vehicles, and animals. This limitation may be partially overcome at the cost of increased hardware complexity by augmenting Doppler sensing with

Authorized licensed use limited to: Indraprastha Institute of Information Technology. Downloaded on July 21,2021 at 13:41:40 UTC from IEEE Xplore. Restrictions apply.

either direction-of-arrival or range processing [40], [41]. Cammenga *et al.* [42] have used both high range resolution capability of ultra wide band (UWB) radar and micro-Doppler information to obtain joint range time-frequency profiles with a view to separate groups of targets.

In this paper, we propose to retain the low cost and complexity of continuous wave radar hardware. Therefore, we adopt signal processing to detect multiple simultaneously moving targets by separating the aggregate backscatter signal into individual components from each target. Algorithmically, signal disaggregation is a single channel source separation problem rather than a classification problem. The algorithm used in this paper is based on sparse coding methods that were recently developed to separate the energy signals from multiple residential electrical appliances into their component signals [43].

Here, we use training data to learn a unique model or dictionary for the micro-Doppler data from each target class. Since dictionary learning is driven by the radar data, its atoms may be better tuned to match the underlying signal. Consequently such learned dictionaries can represent the radar signal in a sparser fashion compared to data-independent transforms like wavelet or Fourier. Once learnt, these dictionaries can be directly used to classify test data from each class. In contrast, in a disaggregation scenario, the dictionaries of all the classes are combined together and the resulting set is used for separating the test aggregate radar signal from multiple targets. Subsequently, the presence of these targets can be detected based on the strength of their corresponding disaggregated micro-Dopplers.

We demonstrate this approach for detecting four indoor movers with a monostatic continuous wave Doppler radar at 7.5 GHz. The target classes are a human walking toward the radar, a human walking away from the radar, and a human walking in a tangential direction before a radar and a table fan (TF). The training micro-Doppler data for learning dictionaries are obtained from measurements of 40 individuals (men and women of varying heights and gaits) and a TF with multiple rotation speeds, orientations, and distances from the radar. The test data were gathered separately for different combinations of humans and fan in single, two, three, and four target scenarios. We use the previously learnt dictionaries to both classify and disaggregate the test data. Our results demonstrate that unlike the classifier that uses the dictionaries to accurately identify only the strongest target returns, the disaggregation algorithm correctly detects multiple targets that are simultaneously moving in the channel in more than 94% of the cases. Subsequent sections of the paper are organized as follows. Section II briefly explains the algorithms used for dictionary learning, classification, and disaggregation. In Section III, we describe the experimental setup and the data collection process. The validation of the proposed method is presented in Sections IV and V concludes the paper.

II. THEORY

There have been several research efforts into representing micro-Dopplers with traditional data-independent dictionaries for classification purposes. In these cases, the dictionary parameters such as the short time window duration, in the case of Fourier, must be set based on the type of target. Hence, when there are multiple targets, the selection of the appropriate parameters for the successful representation of the signal becomes challenging. Dictionary learning presents an alternate method where a set of basis vectors or atoms (dictionaries, $\mathbf{D}$) are used to represent signals $\mathbf{X}$, as shown in (1). Here, each column of $\mathbf{X}$ indicates a time-domain measurement of the radar signal:

$$\mathbf{X} = \mathbf{DZ}. \tag{1}$$

These atoms can be tuned to the underlying signal and hence may yield slightly sparser representations of the signals $\mathbf{Z}$ than the data-independent dictionaries. In essence, dictionary learning from training data $\mathbf{X}$ involves minimizing the objective function $J(\mathbf{D}, \mathbf{Z})$, as shown in the following equation:

$$J(\mathbf{D}, \mathbf{Z}) = \min_{\mathbf{D},\mathbf{Z}} \|\mathbf{X} - \mathbf{DZ}\|_F^2 + \lambda \|\mathbf{Z}\|_0 . \tag{2}$$

Here, $\|.\|_0$ is the l_0-norm that provides a count of the number of nonzero elements in coefficients $\mathbf{Z}$. The optimization is done through a two-staged procedure where atoms of dictionary and coefficients are updated through two alternating minimization operations as described ahead.

A. Two-Stage Implementation of Dictionary Learning

We consider N number of M-dimensional training signals denoted by $\mathbf{X} = [x_1 \ldots x_N]$, where $x_n \in R^{M\times 1}$. Dictionaries are learnt from $\mathbf{X}$ in a two-staged iterative procedure. First, the dictionaries are initialized using randomly selected training signals such that $\mathbf{D} \in \mathbf{R}^{M\times P}$ is overcomplete (where the number of atoms P is greater than the signal dimension M).

1) *Sparse Coding Stage:* In order to ensure sparse representation of $\mathbf{X}$, we impose the following constraint on the coefficients $\mathbf{Z}$, as shown in the following equation:

$$\mathbf{Z} = \min_{\mathbf{Z}} \|\mathbf{X} - \mathbf{DZ}\|_F^2 \text{ s.t. } \|\mathbf{Z}\|_0 < \tau \tag{3}$$

The sparsity level is controlled by parameter τ. Unfortunately,\ l_0-minimization is NP-hard [44]. Compressed sensing has demonstrated that we can replace the l_0-norm with l_1-norm, as shown in (4), and still ensure sparsity:

$$\mathbf{Z} = \min_{\mathbf{Z}} \|\mathbf{X} - \mathbf{DZ}\|_F^2 + \lambda \|\mathbf{Z}\|_1 . \tag{4}$$

Here, $\lambda \in R$ is a regularization parameter that controls the tradeoff between the level of sparsity in $\mathbf{Z}$ and the error in data fitting. The formulation in (4) is a convex problem, which we solve using the iterative soft thresholding algorithm (ISTA) algorithm suggested by Selesnick [45].

2) *Dictionary Update Stage:* Once the sparse coefficients are obtained, the dictionary is updated using a least squares approach [46], as shown in (5). Columns of

Authorized licensed use limited to: Indraprastha Institute of Information Technology. Downloaded on July 21,2021 at 13:41:40 UTC from IEEE Xplore. Restrictions apply.

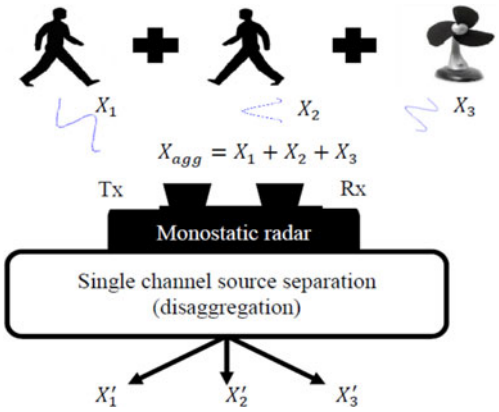

Fig. 1. Single channel source separation of radar signals from multiple targets.

dictionary are normalized to have norm less than unity:

$$\boldsymbol{D} = \min_{\mathbf{D}} \|\mathbf{X} - \mathbf{D}\mathbf{Z}\|_F^2$$
$$\text{s.t.} \left\|d_p\right\|_2^2 \leq 1, \forall p = 1, 2, \ldots P. \tag{5}$$

This two-staged process is iterated until $J(\mathbf{D}, \mathbf{Z})$ converges or reaches a very low tolerance level.

If there are I target classes, the corresponding dictionaries $\mathbf{D}_i$ are learnt for each ith class using this procedure. Once learnt, the dictionaries can be used either directly for classification as described in Section II-C or can be used to disaggregate or separate the superposed radar backscattered signals from multiple moving targets as described in Section II-B. The limitation of classification algorithm is that the aggregate signal is classified or assigned to just a single class. In contrast, the disaggregation algorithm enables the aggregate signal to be assigned across multiple classes.

B. Sparse Coding Based Disaggregation

If there are multiple movers in the propagation channel, the received signal at the radar receiver is the aggregate $\mathbf{X}_{\text{agg}}$ from all of these targets, as shown in Fig. 1:

$$\mathbf{X}_{\text{agg}} = \Sigma_{i=1}^{I} \mathbf{X}_i. \tag{6}$$

Here, $\mathbf{X}_i$ are the radar signals from ith target class. Our aim is to disaggregate $\mathbf{X}_{\text{agg}}$ into the constituent components $\mathbf{X}'_1 \ldots \mathbf{X}'_I$ belonging to I different classes. First, the dictionaries from all the classes are combined together to form a set: $\mathbf{D}_{(1:I)} = [\mathbf{D}_1 \ldots \mathbf{D}_I]$. Then, we solve for the sparsest solution $\hat{\mathbf{Z}}_{1:I}$ for each class i, as shown in the following equation:

$$\hat{\mathbf{Z}}_{1:I} = \min_{\hat{\mathbf{Z}}_{1:I}} \left\|\mathbf{X}_{\text{agg}} - \mathbf{D}_{1:I}\hat{\mathbf{Z}}_{1:I}\right\|_F^2 + \lambda_1 \left\|\hat{\mathbf{Z}}_{1:I}\right\|_1. \tag{7}$$

The intuition behind this technique is as follows. If $\mathbf{D}_i$ is trained to reconstruct $\mathbf{X}_i$, then it will be able to reconstruct $\mathbf{X}'_i = \mathbf{D}_i\hat{\mathbf{Z}}_i$, which is the ith portion of the aggregate signal better than any other $\mathbf{D}_j$ for $j \neq i$. The assumption here is that the dictionaries learnt for specific classes are discriminative and have less coherence between them. If this assumption does not yield satisfactory results, an additional

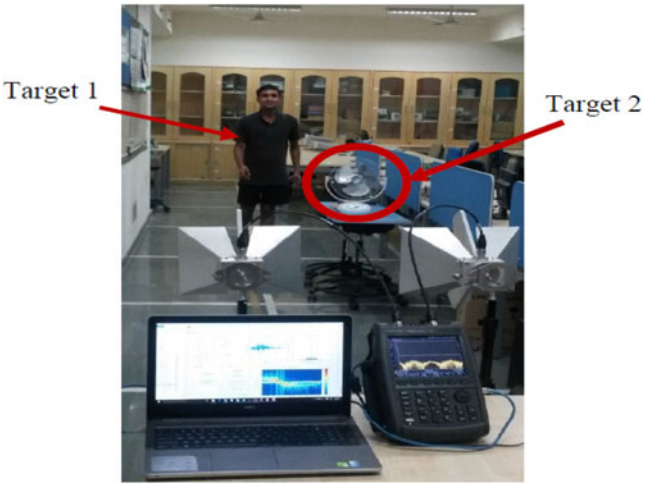

Fig. 2. Experimental setup using FieldFox VNA and two horn antennas as monostatic radar at 7.5 GHz for detecting one or more targets (human walking toward radar and human walking away from radar and TF).

constraint can be imposed on the dictionary learning algorithm to ensure that the discrimination across dictionaries is maximized [47], [48]. In our case, this was found to not be necessary. Most of the active elements of $\hat{\mathbf{Z}}_{1:I}$ should be located in $\hat{\mathbf{Z}}_i$ where i is the class to which the signal belongs. Therefore, once the signal has been disaggregated, the target i is detected if the strength $\left\|\hat{\mathbf{Z}}_i\right\|_2$ is above a predefined threshold (γ_T). In other words, ideally, each target signal is expected to lie in its own class subspace and all the class subspaces are nonoverlapping.

C. Sparse Representation Based Classification

If we wish to simply classify the aggregate signal into one of the I classes, we can directly use the learnt dictionaries $\mathbf{D}_i$ in the sparse representation based classifier (SRC) [49]. The test signal will be assigned to the class $\hat{i}$ having the least error amongst all class representations, as shown in the following equation:

$$\hat{i} = \min_i \left\|\mathbf{X}_{\text{agg}} - \mathbf{D}_i\hat{\mathbf{Z}}_i\right\|_2^2 \ \forall i = 1, 2, \ldots I. \tag{8}$$

The classification algorithm is therefore not suited for detecting multiple targets that are simultaneously present in the channel. Note that in prior works the test signal was assumed to consist of radar backscatter from only a single target. Any backscatter from other moving objects in the background were simply treated as noise. In contrast, we consider the test signal to be the aggregate backscatter from multiple targets ($\mathbf{X}_{\text{agg}}$) and our objective is to detect all the movers.

III. EXPERIMENTAL SETUP

The experiments were performed on four commonly occurring classes of indoor moving targets: Human walking toward the radar (FH), away from radar (BH), and walking in tangential direction before the radar (SH) and TF. A monostatic continuous wave Doppler radar configuration was operated at 7.5 GHz, as shown in Fig. 2. Our

Authorized licensed use limited to: Indraprastha Institute of Information Technology. Downloaded on July 21,2021 at 13:41:40 UTC from IEEE Xplore. Restrictions apply.

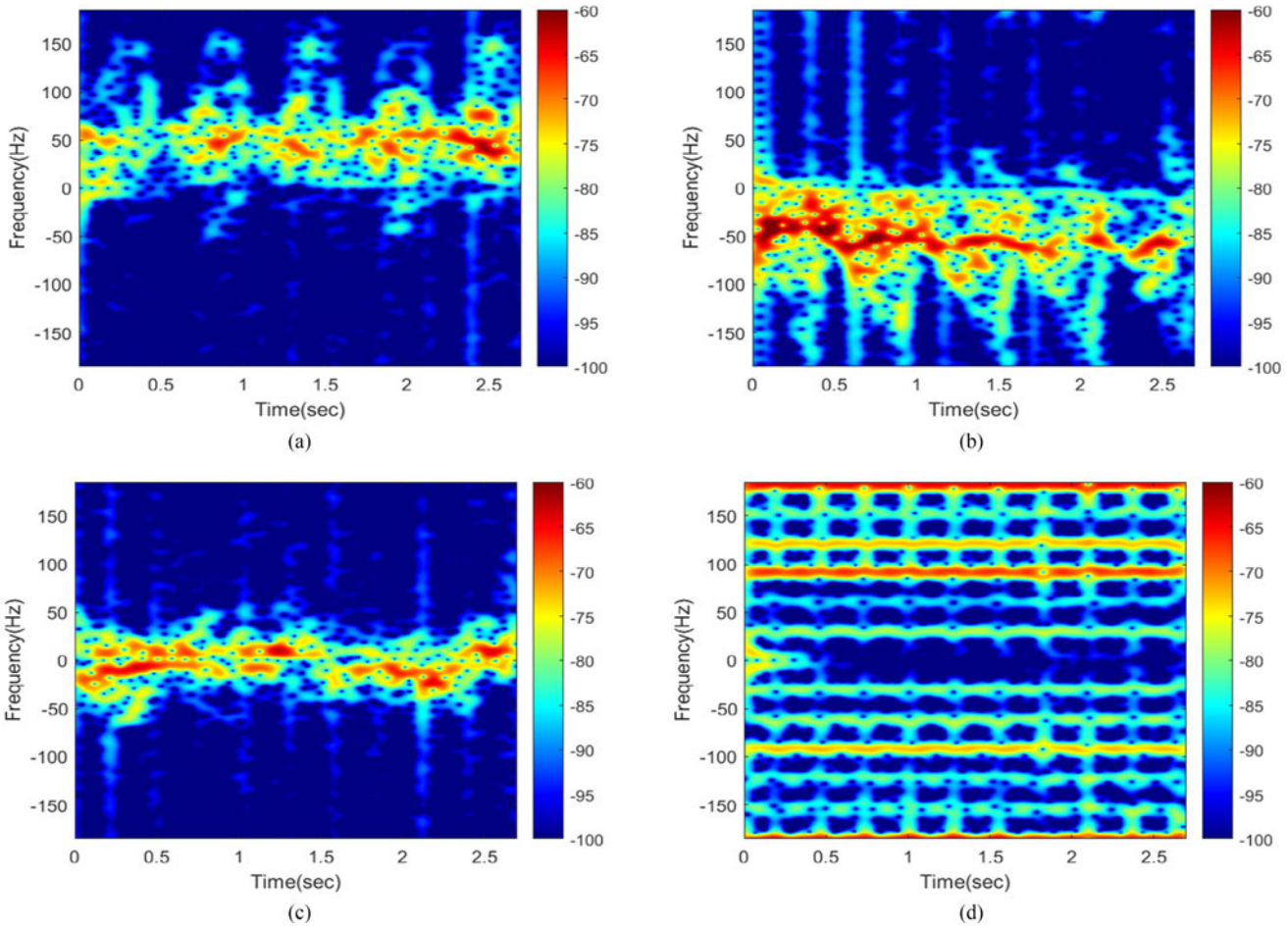

Fig. 3. Doppler spectrogram of (a) human walking away from radar, (b) human walking toward radar, (c) human walking tangentially before the radar, and (d) rotating TF generated with monostatic radar at 7.5 GHz.

system comprised of two linearly polarized double-ridged waveguide horn antennas (HF907), separated by a distance of 50 cm, and N9926A FieldFox vector network analyzer (VNA). The backscattered radar returns from targets were gathered from time-domain S_{21} measurements of the VNA, which were subsequently processed in MATLAB. Our radar system is capable of a dynamic range of approximately 100 dB with a noise floor of -120 dBm. The measurements were conducted in an indoor environment under line-of-sight conditions. The targets always moved within the field-of-view of the radar antennas. The duration of each measurement was 2.7 s with 1000 samples. Each measurement was further repeated five times resulting in a signal of size $[1000 \times 5]$. Measurement data were gathered from 40 human subjects (with varying gaits, heights, and velocities) and a TF (with different angular velocities, distances, and orientations with respect to the radar). The human subjects moved roughly between 1 and 9 m in front of the radar. These data were gathered in single, two, three, and four targets scenarios. The complete dataset and its detailed description is available in the appendix.

Fig. 3 shows the Doppler spectrograms generated from measured data gathered from a single target scenario using short time-frequency transform. When the human is walking away from the radar (BH), the Dopplers, as shown in Fig. 3(a), are mostly negative except for the back swing from the arms and legs. The strength of the Dopplers decrease with time as the distance from the radar increases. On the other hand, the Dopplers are mostly positive, in Fig. 3(b), when the human is walking toward the radar (FH). The Doppler spread is directly a function of the velocity and height of the human since the feet give rise to the maximum absolute values of Dopplers. When the human is walking tangentially before the radar (SH), the Dopplers are less pronounced, as shown in Fig. 3(c), though their strengths are similar to the FH and BH cases. This is due to the low Doppler shift that arises from the target's cross line-of-sight motion with respect to the radar. The periodicity in the Dopplers correspond to the gait of the human. Fig. 3(d) shows the spectrogram due to the three rotating blades of the TF. The Dopplers here are a function of the blade length, the angular velocity, and the orientation of the fan. Due to low sampling frequency limits imposed by the VNA, aliasing can be observed in the spectrogram. However, this is ignored since the purpose of through-wall radars is mostly to detect humans.

Authorized licensed use limited to: Indraprastha Institute of Information Technology. Downloaded on July 21,2021 at 13:41:40 UTC from IEEE Xplore. Restrictions apply.

TABLE I
Disaggregation Algorithm for Detection of Multiple Target Classes

Input: Training data matrix $\mathbf{X}_i^{Tr} \in \mathbf{R}^{M\times N}$, from I individual classes for $i = 1, 2, \ldots I$, $\lambda \in R$ is a regularization parameter.

Stage 1: Learning class specific dictionaries for $i = 1, 2 \ldots I$

Loop until convergence

$$\{\mathbf{Z}_i\} = \min_{\mathbf{Z}_i} \left\|\mathbf{X}_i^{Tr} - \mathbf{D}_i\mathbf{Z}_i\right\|_F^2 + \lambda \left\|\mathbf{Z}_i\right\|_1$$

$$\{\mathbf{D}_i\} = \min_{\mathbf{D}_i} \left\|\mathbf{X}_i^{Tr} - \mathbf{D}_i\mathbf{Z}_i\right\|_F^2 s.t \left\|d_{pi}\right\|_2^2 \leq 1$$

End

Stage 2: Disaggregation of $\mathbf{X}_{agg}$ using learnt dictionaries from I different classes concatenated together, $\mathbf{D}_{1:I} = [\mathbf{D}_1 \ldots \mathbf{D}_I]$, $\lambda_1 \in R$ is a regularization parameter.

(a) Sparse Coding

$$\hat{\mathbf{Z}}_{1:I} = \min_{\hat{\mathbf{Z}}_{1:I}} \left\|\mathbf{X}_{agg} - \mathbf{D}_{1:I}\hat{\mathbf{Z}}_{1:I}\right\|_F^2 + \lambda_1 \left\|\hat{\mathbf{Z}}_{1:I}\right\|_1$$

(b) Detection based on strength of sparse coefficients $\hat{\mathbf{Z}}_i$, γ_T is the defined threshold

$$\hat{\mathbf{Z}}_i = \left\{ \begin{array}{l} \hat{\mathbf{Z}}_i \; if \;\; \left\|\hat{\mathbf{Z}}_i\right\|_2 \geq \gamma_T \\ 0 \; if \;\; \left\|\hat{\mathbf{Z}}_i\right\|_2 < \gamma_T \end{array} \right\}$$

(c) Reconstruction of disaggregated signal

$$\mathbf{X}_i' = \mathbf{D}_i\hat{\mathbf{Z}}_i$$

A. Training Data

About 75% of the measurement data gathered in the single target scenario for the four target classes ($\mathbf{X}_{\text{FH}}^{\text{TR}}$, $\mathbf{X}_{\text{BH}}^{\text{TR}}$, $\mathbf{X}_{\text{SH}}^{\text{TR}}$ and $\mathbf{X}_{\text{TF}}^{\text{TR}}$) were used for training purposes. As a result, the training signal matrix for both the target types—humans and TF is of size [1000 × 150]. During stage 1 of Table I, class specific dictionaries ($\mathbf{D}_{\text{FH}}$, $\mathbf{D}_{\text{BH}}$, $\mathbf{D}_{\text{SH}}$, and $\mathbf{D}_{\text{TF}}$) are learnt from the training data corresponding to the four targets. We examined dictionaries of size [1000 × 500] for all the target types, for four different values of $\lambda = 0.0001, 0.001, 0.01, 0.1$, We finally adopted the dictionaries with the least error of signal representation.

B. Test Data

Our training and test scenarios are not identical. They differ in the following key ways: First, the test data were gathered from a different set of subjects than the training data; second, the data $\mathbf{X}_{\text{agg}}$ were gathered in two, three, and four target scenarios (as opposed to the single target scenario for training data). In both the training and test cases, the humans and fans were placed in different locations and orientations with respect to the radar. Then, $\mathbf{X}_{\text{agg}}$ and the concatenated dictionaries were used as input to the sparse coding based disaggregation algorithm described in stage 2 of Table I to obtain constituent signal components from different movers. A target *i* was detected if the strength of disaggregated coefficient $||\hat{\mathbf{Z}}_i||_2$ was greater than a predefined threshold value for human targets and for TF, which was determined empirically from the noise floor of the measurements and the average radar cross section of the targets. In the absence of prior works on disaggregation of micro-Doppler data, we compare the performance of the algorithm with the classification algorithm described in (8). Each test case is assigned to the class *i* that gives rise to the minimum residue between the test data $\mathbf{X}_{\text{agg}}$ and $\mathbf{D}_i$, $\mathbf{Z}_i$. Thus, the classification algorithm can be used to identify the presence of only a single target in the channel. Strictly speaking, the disaggregation and classification algorithms therefore have different objectives and only the former is suited for the simultaneous detection of multiple targets.

IV. RESULTS

In this section, we examine the performance of the disaggregation and classification algorithms.

A. Doppler Spectrograms of Disaggregated Signals

The dictionary learning based algorithm is a supervised learning technique where the target classes must be known prior to detection. We consider a three target class scenario where the algorithm must detect the presence of one or more of three targets (FH, BH, or TF) on the basis of disaggregation of backscatter signals. First, we qualitatively compare the Doppler spectrograms generated from the disaggregated components with the previously shown spectrograms in Fig. 3. The Doppler spectrograms in all of the cases are generated with the short time Fourier transform with a dwell time of 54 ms. In the first case, we consider a two target scenario a human walking toward the radar (FH) and a TF are present in the channel. The radar cross section of the human is greater than that of the fan. The spectrogram in Fig. 4(a) shows radar backscatter from both the targets with corresponding micro-Doppler features. The micro-Dopplers overlap at certain frequencies. If these aggregated data are directly used for classification, it is quite likely that the target will be assigned to class FH due to the strength of its returns. Fig. 4(b)–(d) shows the spectrograms generated from the disaggregated components and the advantages of the proposed algorithm. We clearly observe targets belonging to the classes FH [see Fig. 4(b)] and TF [see Fig. 4(d)] while there is no target belonging to the class BH [see Fig. 4(c)]. Note that the strength of the disaggregated components [Fig. 4(a) and (c)] slightly differ from what is observed in the aggregate signal [see Fig. 4(a)]. This may be attributed to the interference between the signals belonging to the different classes in the

Authorized licensed use limited to: Indraprastha Institute of Information Technology. Downloaded on July 21,2021 at 13:41:40 UTC from IEEE Xplore. Restrictions apply.

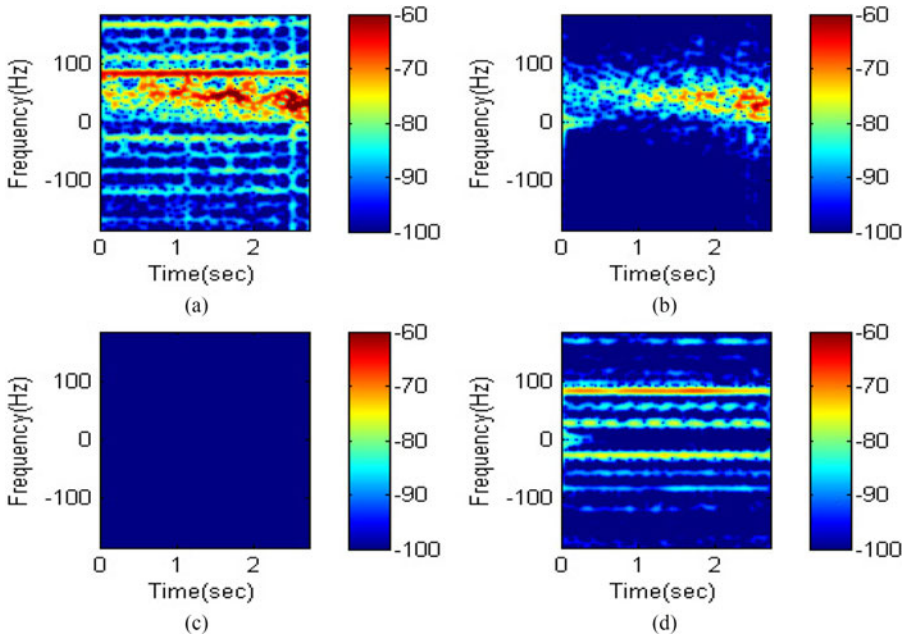

Fig. 4. Doppler spectrogram of (a) aggregate micro-Doppler from a human walking toward the radar and a rotating TF, (b) disaggregated micro-Doppler of human walking toward radar (indicating presence of target), (c) disaggregated micro-Doppler of human walking away from radar (indicating absence of target), and (d) disaggregated return of rotating TF (indicating presence of target).

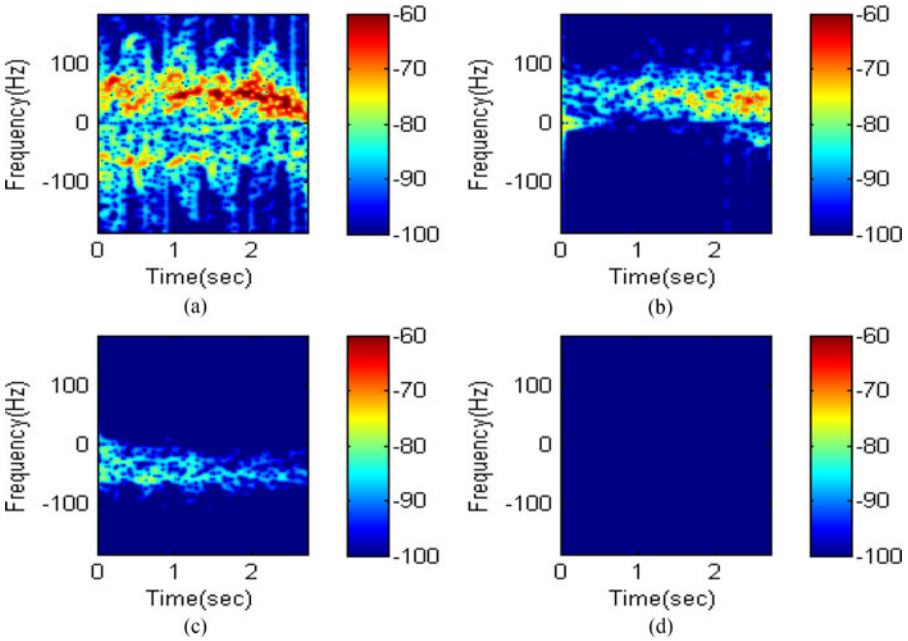

Fig. 5. Doppler spectrogram of (a) aggregate micro-Doppler from two humans, one walking toward the radar and one walking away from radar, (b) disaggregated micro-Doppler of human walking toward radar (indicating presence of target), (c) disaggregated micro-Doppler of human walking away from radar (indicating presence of target), and (d) disaggregated return of rotating TF (indicating absence of target).

aggregate signal. Another two target scenario is when two humans are walking one toward and the other away from the radar (FH and BH). This is a more challenging scenario since the radar cross sections of the two humans are comparable. The spectrogram shown in Fig. 5(a), clearly indicates both positive and negative micro-Dopplers emanating from the two targets. There is still some overlap between the micro-Dopplers from the back swing of the arms and legs. Due to the similarity in the strength of the returns from both the targets, the classification algorithm, based on these aggregate data, is quite likely to be confused between classes FH and BH. The spectrograms from the disaggregated components, on the other hand, clearly indicate the presence of FH [see Fig. 5(b)] and BH [see Fig. 5(c)], and the absence of TF [see Fig. 5(d)]. The disaggregation algorithm, however, does seem to not correctly pick out the highest Dopplers

Authorized licensed use limited to: Indraprastha Institute of Information Technology. Downloaded on July 21,2021 at 13:41:40 UTC from IEEE Xplore. Restrictions apply.

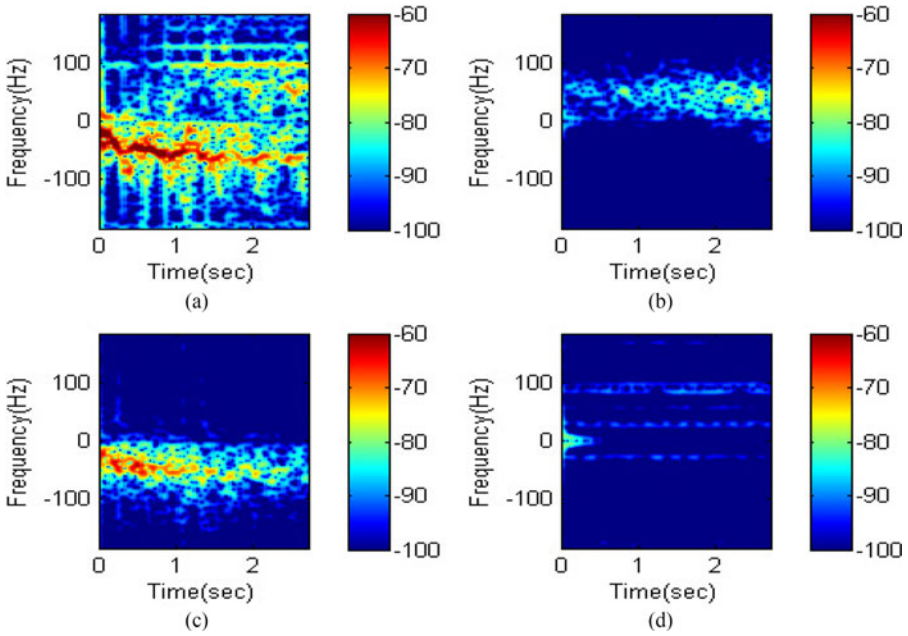

Fig. 6. Doppler spectrogram of (a) aggregate micro-Doppler from two humans, one walking toward the radar and one walking away from radar and a rotating TF, (b) disaggregated micro-Doppler of human walking toward radar (indicating presence of target), (c) disaggregated micro-Doppler of human walking away from radar (indicating presence of target), and (d) disaggregated return of rotating TF (indicating presence of target).

TABLE II
Classification of Radar Data Across Human Walking Toward Radar (FH), Human Walking Away From Radar (BH) and Rotating TF Classes

Cases(T/P)	FH (%)	BH (%)	TF (%)
Single target-FH	92	8	0
Single target-BH	6	94	0
Single target-TF	20	10	70
Two targets-FH + TF	82	10	8
Two targets-BH + TF	6	84	10
Two targets-FH + BH	52.5	47.5	0
Three targets-FH + BH + TF	40	60	0

Here P is the predicted class and T is the true class.

arising from the motion of the feet. This may be due to the variation in the training data corresponding to humans of different heights. Finally, we consider a three target scenario when radar returns from all three moving targets (FH, BH, and TF) are present. The spectrogram of aggregate signals, shown in Fig. 6(a), indicates that the aggregate data may be confused mostly between FH and BH since the returns from TF are weaker. In contrast, the spectrograms of the disaggregated components shown in Fig. 6(b)–(d) indicates that all three targets will be correctly detected.

B. Classification Results for SRC

We classified the measurement data belonging to the single, two, and three target scenarios into one of three classes (FH, BH, or TF) using the SRC algorithm discussed in Section II-C. The results are presented in Table II. In the single target scenario case (FH/BH/TF), the classifier most often picks the correct class for the target. The average accuracy for this scenario is 85%. This confirms the hypothesis that micro-Doppler signatures are useful tools for classifying moving targets. For comparison purposes, we also applied the single target data with LC-KSVD algorithm reported in [50] and obtained 75% classification accuracy. The classifier is mostly confused between the FH and BH classes. Next, we examine the performance of the algorithm when multiple targets are present in the channel. The results for the two targets scenarios FH + TF and BH + TF, cases show that the classification performance is skewed toward the targets with the stronger radar cross section (humans). In other words, the returns from the weaker targets (TF) are treated as noise by the algorithm. On the other hand, when both the targets are humans (FH + BH), and therefore, of comparable radar cross sections, the classifier pretty evenly distributes the cases between them. In the case of the three target scenario (FH + BH + TF), the classification accuracy is again skewed toward the stronger targets (humans) in favor of the weaker TF. These results show that the classifier can accurately detect the strongest target when all other moving objects in the background give rise to much weaker returns. The performance of the classifier deteriorates when there are multiple targets with comparable backscatter.

C. Detection Results After Disaggregation of Micro-Doppler Data

The disaggregation algorithm, unlike the classification algorithm, is meant for the detection of multiple targets. This time, we consider measurement data from four target

Authorized licensed use limited to: Indraprastha Institute of Information Technology. Downloaded on July 21,2021 at 13:41:40 UTC from IEEE Xplore. Restrictions apply.

TABLE III
Detection Based on Disaggregation of Data From Human Walking Toward Radar (FH) and Human Walking Away From Radar (BH) and Rotating TF

Scenario(T/P)	True detections (%)	Missed detections (%)	False alarms (%)
Single target-FH	FH:100 BH:NA TF:NA	FH:0 BH:NA TF:NA	FH:NA BH:4 TF:14
Single target-BH	FH:NA BH:100 TF:NA	FH:NA BH:0 TF:NA	FH:12 BH:NA TF:8
Single target-SH	FH:NA BH:NA TF:NA SH:100	FH:NA BH: NA TF:NA SH:0	FH:0 BH:0 TF:0 SH:NA
Single target-TF	FH:NA BH:NA TF:94	FH:NA BH: NA TF:6	FH:2 BH:0 TF:NA
Two targets-FH + TF	FH:88 BH:NA TF:94	FH:12 BH: NA TF:6	FH:NA BH:12 TF:NA
Two targets-BH + TF	FH:NA BH:94 TF:96	FH:NA BH:6 TF:4	FH:28 BH:NA TF:NA
Two targets-FH + BH	FH:87.5 BH:80 TF:NA	FH:12.5 BH:20 TF:NA	FH:NA BH:NA TF:52.5
Two targets-SH + TF	FH:NA BH:NA TF:98 SH:100	FH:NA BH: NA TF:2 SH:0	FH:22 BH:0 TF:NA SH:NA
Three targets-FH + BH + TF	FH:95 BH:90 TF:90	FH:5 BH:10 TF:10	FH:NA BH:NA TF:NA
Three targets-SH + FH + TF	FH:95 BH:NA TF:100 SH:100	FH:5 BH: NA TF:0 SH:0	FH:NA BH:0 TF:NA SH:NA
Three targets-SH + BH + TF	FH:NA BH:95 TF:100 SH:100	FH:NA BH: 5 TF:0 SH:0	FH:25 BH:NA TF:NA SH:NA
Four targets-FH + BH + TF + SH	FH:87.5 BH:67.5 TF:100 SH:100	FH:12.5 BH: 32.5 TF:0 SH:0	FH:NA BH:NA TF:NA SH:NA
Average	94	6	11

class labels (FH, BH, SH, and TF). The resultant detection accuracies for the single, two, three, and four targets scenarios are presented in Table III. We achieve an average true detection accuracy of 98.5% for the four single target scenarios (FH/BH/SH/TF) while the false alarm was 4.4%. When we examine the two target scenarios—we are now able to detect both the targets in 88% of the FH + TF cases, 94% in BH + TF cases, 80% in FH + BH, and 98% in SH + TF cases. This result demonstrates the usefulness of the disaggregation algorithm when compared to the classification algorithms for the detection of multiple targets. We were able to detect the weak target (TF) in the presence of strong targets (FH, BH, and SH). We were also able to detect two targets of comparable returns. However, the limitation is that we have a high false alarm rate. This is because when two targets are present, there is a high probability of the overlap of the signals in the frequency domain. We investigate the performance of the proposed

Authorized licensed use limited to: Indraprastha Institute of Information Technology. Downloaded on July 21,2021 at 13:41:40 UTC from IEEE Xplore. Restrictions apply.

TABLE IV
Dataset Description

Target scenario and description	Target parameters	Training Data	Test Data
Single target- FH, BH, SH	Number of subjects: 40 Target heights: 5 to 6 Target velocities: 0.6 to 1.5 m/s Number of measurements = 200 (5 measurements from each of the 40 subjects)	150 (5 measurements from of the 30 subjects)	50 (5 measurements from of the 10 subjects)
Single target- TF	Number of fans: 1 Angular velocities: 1400 r/min, 2000 and 2600 r/min Locations from the radar: 8 Number of measurements = 240 (10 measurements from each of the 24 cases)	150 (10 measurements from each of the 15 cases)	50 (10 measurements from each of the 5 cases)
Two targets- FH + TF, BH + TF, SH + TF	Number of humans: 5 Number of fans: 1 Locations of fan: 2 Number of measurements: 50 (5 measurements from each of the 5 × 2 cases)	0 (No training data)	50 (All measurement data are used for testing)
Two targets- FH + BH	Number of humans walking toward radar: 2 Number of humans walking away from radar: 2 Number of measurements: 40 (10 measurements from each of the 4 cases)	0 (No training data)	40 (All measurement data are used for testing)
Three targets- FH + BH + TF, FH + SH + TF, BH + SH + TF	Number of humans: 2 Number of fans: 1 Number of measurements: 20 (10 measurements from each of the 2 cases)	0 (No training data)	20 (All measurement data are used for testing)
Four targets- FH + BH + SH + TF	Number of humans: 3 Number of fans: 1 Number of measurements: 20 (10 measurements from each of the 2 cases)	0 (No training data)	20 (All measurement data are used for testing)

algorithm in the three target scenario. When three targets move simultaneously, it is almost impossible to not have micro-Doppler overlap. Despite this, the algorithm detects all three targets in 96% of the cases. Obviously, the humans are favored (more than 95% detection accuracy) since they have the stronger radar cross sections. Finally, we tested our approach in four target scenario where FH, BH, SH, and TF moved simultaneously in the same channel. Here, detection accuracies for SH and TF are 100% whereas for FH it is 87.5%. For the case of BH the accuracy dropped to 67.5%, this can be attributed to the weaker return signals in some of the BH cases in comparison to SH and FH.

V. CONCLUSION

We used supervised dictionary learning techniques to represent micro-Doppler from dynamic targets. These dictionaries result in sparser representations of the radar signals than the classical data-independent dictionaries such as wavelets or Fourier. Hence, they can be used to accurately classify targets in single target scenarios. However, the real advantage of these dictionaries is realized in multi-target scenarios. The dictionaries can be used to disaggregate the superposed radar signals obtained from multiple targets into individual components. This enables the detection of weak targets in the presence of stronger returns. We have evaluated the algorithms performance in detecting four indoor targets, three humans, and a TF. The overall detection accuracy across single, two, three, and four targets scenarios is 94% and the false alarm rate is 11%. Note that the false alarm values are not a function of the threshold selected in the algorithm and are instead due to the limitations in the dictionary learning algorithm. The discrimination capability of the dictionaries is governed by the degree of overlap in the micro-Dopplers. In all of the above-mentioned cases, we have assumed that each target class (FH, BH, SH, or TF) consists of only a single target. The algorithm can be applied to disaggregate data where each class may comprise of several targets. However, we will need to incorporate additional complexity (hardware or software) to determine the actual number of targets within each class.

APPENDIX

See Table IV.

Authorized licensed use limited to: Indraprastha Institute of Information Technology. Downloaded on July 21,2021 at 13:41:40 UTC from IEEE Xplore. Restrictions apply.

ACKNOWLEDGMENT

The authors would like to thank Prof. A. Majumdar for useful discussions regarding dictionary learning.

REFERENCES

[1] V. C. Chen, F. Li, S.-S. Ho, and H. Wechsler
Analysis of micro-Doppler signatures
IEE Proc., Radar, Sonar Navig., vol. 150, no. 4, pp. 271–276, 2003.

[2] V. C. Chen, F. Li, S.-S. Ho, and H. Wechsler
Micro-doppler effect in radar: Phenomenon, model, and simulation study
IEEE Trans. Aerosp. Electron. Syst., vol. 42, no. 1, pp. 2–21, Jan. 2006.

[3] A. Ghaleb, L. Vignaud, and J. Nicolas
Micro-doppler analysis of wheels and pedestrians in isar imaging
IET Signal Process., vol. 2, no. 3, pp. 301–311, 2008.

[4] J. A. Nanzer and R. L. Rogers
Bayesian classification of humans and vehicles using micro-doppler signals from a scanning-beam radar
IEEE Microw. Wireless Compon. Lett., vol. 19, no. 5, pp. 338–340, May 2009.

[5] Y. Li, L. Du, and H. Liu
Hierarchical classification of moving vehicles based on empirical mode decomposition of micro-doppler signatures
IEEE Trans. Geosci. Remote Sens., vol. 51, no. 5, pp. 3001–3013, May 2013.

[6] L. Du, L. Li, B. Wang, and J. Xiao
Micro-doppler feature extraction based on time-frequency spectrogram for ground moving targets classification with low-resolution radar
IEEE Sensors J., vol. 16, no. 10, pp. 3756–3763, May 2016.

[7] R. Nepal, J. Cai, and Z. Yan
Micro-doppler radar signature identification within wind turbine clutter based on short-CPI airborne radar observations
IET Radar, Sonar Navig., vol. 9, no. 9, pp. 1268–1275, 2015.

[8] T. Thayaparan, S. Abrol, E. Riseborough, L. Stankovic, D. Lamothe, and G. Duff
Analysis of radar micro-doppler signatures from experimental helicopter and human data
IET Radar, Sonar Navig., vol. 1, no. 4, pp. 289–299, 2007.

[9] M. K. Baczyk, P. Samczyński, K. Kulpa, and J. Misiurewicz
Micro-doppler signatures of helicopters in multistatic passive radars
IET Radar, Sonar Navig., vol. 9, no. 9, pp. 1276–1283, 2015.

[10] P. Molchanov, K. Egiazarian, J. Astola, A. Totsky, S. Leshchenko, and M. P. Jarabo-Amores
Classification of aircraft using micro-doppler bicoherence-based features
IEEE Trans. Aerosp. Electron. Syst., vol. 50, no. 2, pp. 1455–1467, Apr. 2014.

[11] V. C. Chen and H. Ling
Time-Frequency Transforms for Radar Imaging and Signal Analysis. Norwood, MA, USA: Artech House, 2002.

[12] Z. Zhang, P. O. Pouliquen, A. Waxman, and A. G. Andreou
Acoustic micro-doppler radar for human gait imaging
J. Acoust. Soc. Amer., vol. 121, no. 3, pp. EL110–EL113, 2007.

[13] Y. Kim and H. Ling
Human activity classification based on micro-doppler signatures using a support vector machine
IEEE Trans. Geosci. Remote Sens., vol. 47, no. 5, pp. 1328–1337, May 2009.

[14] B. G. Mobasseri and M. G. Amin
A time-frequency classifier for human gait recognition
Proc. SPIE, vol. 7306, 2009, Art. no. 730628.

[15] I. Orović, S. Stanković, and M. Amin
A new approach for classification of human gait based on time-frequency feature representations
Signal Process., vol. 91, no. 6, pp. 1448–1456, 2011.

[16] J. Park *et al.*
Simulation and analysis of polarimetric radar signatures of human gaits
IEEE Trans. Aerosp. Electron. Syst., vol. 50, no. 3, pp. 2164–2175, Jul. 2014.

[17] M. G. Amin, F. Ahmad, Y. D. Zhang, and B. Boashash
Human gait recognition with cane assistive device using quadratic time–frequency distributions
IET Radar, Sonar Navig., vol. 9, no. 9, pp. 1224–1230, 2015.

[18] B. Lyonnet, C. Ioana, and M. G. Amin
Human gait classification using microdoppler time-frequency signal representations
In *Proc. IEEE Radar Conf.*, 2010, pp. 915–919.

[19] R. M. Narayanan, M. C. Shastry, P.-H. Chen, and M. Levi
Through-the-wall detection of stationary human targets using doppler radar
Progr. Electromagn. Res. B, vol. 20, pp. 147–166, 2010.

[20] D. Fairchild and R. Narayanan
Classification of human motions using empirical mode decomposition of human micro-doppler signatures
IET Radar, Sonar Navig., vol. 8, no. 5, pp. 425–434, 2014.

[21] F. Fioranelli, M. Ritchie, and H. Griffiths
Classification of unarmed/armed personnel using the netrad multistatic radar for micro-doppler and singular value decomposition features
IEEE Geosci. Remote Sens. Lett., vol. 12, no. 9, pp. 1933–1937, Sep. 2015.

[22] F. Fioranelli, M. Ritchie, and H. Griffiths
Aspect angle dependence and multistatic data fusion for micro-Doppler classification of armed/unarmed personnel
IET Radar, Sonar Navig., vol. 9, no. 9, pp. 1231–1239, 2015.

[23] J. Bryan, J. Kwon, N. Lee, and Y. Kim
Application of ultra-wide band radar for classification of human activities
IET Radar, Sonar Navig., vol. 6, no. 3, pp. 172–179, 2012.

[24] M. G. Anderson and R. L. Rogers
Micro-Doppler analysis of multiple frequency continuous wave radar signatures
Proc. SPIE, vol. 6547, 2007, Art. no. 65470A.

[25] S. Björklund, H. Petersson, A. Nezirovic, M. B. Guldogan, and F. Gustafsson
Millimeter-wave radar micro-Doppler signatures of human motion
In *Proc. Int. Radar Symp.*, 2011, pp. 167–174.

[26] A. Balleri, K. Chetty, and K. Woodbridge
Classification of personnel targets by acoustic micro-Doppler signatures
IET Radar, Sonar Navig., vol. 5, no. 9, pp. 943–951, 2011.

[27] D. P. Fairchild and R. M. Narayanan
Micro-Doppler radar classification of human motions under various training scenarios
Proc. SPIE, vol. 8734, 2013, Art. no. 873407.

[28] T. Thayaparan, L. Stanković, and I. Djurović
Micro-Doppler-based target detection and feature extraction in indoor and outdoor environments
J. Franklin Inst., vol. 345, no. 6, pp. 700–722, 2008.

[29] Y. Kim, S. Ha, and J. Kwon
Human detection using Doppler radar based on physical characteristics of targets
IEEE Geosci. Remote Sens. Lett., vol. 12, no. 2, pp. 289–293, Feb. 2015.

Authorized licensed use limited to: Indraprastha Institute of Information Technology. Downloaded on July 21,2021 at 13:41:40 UTC from IEEE Xplore. Restrictions apply.

[30] J. Zabalza, C. Clemente, G. Di Caterina, J. Ren, J. J. Soraghan, and S. Marshall
Robust PCA micro-Doppler classification using SVM on embedded systems
IEEE Trans. Aerosp. Electron. Syst., vol. 50, no. 3, pp. 2304–2310, Jul. 2014.

[31] F. H. C. Tivive, S. L. Phung, and A. Bouzerdoum
Classification of micro-Doppler signatures of human motions using log-gabor filters
IET Radar, Sonar Navig., vol. 9, no. 9, pp. 1188–1195, 2015.

[32] V. C. Chen
Spatial and temporal independent component analysis of micro-Doppler features
In *Proc. IEEE Int. Radar Conf*, 2005, pp. 348–353.

[33] C.-P. Lai, R. Narayanan, Q. Ruan, and A. Davydov
Hilbert–huang transform analysis of human activities using through-wall noise and noise-like radar
IET Radar, Sonar Navig., vol. 2, no. 4, pp. 244–255, 2008.

[34] C. Cai, W. Liu, J. S. Fu, and Y. Lu
Radar micro-Doppler signature analysis with HHT
IEEE Trans. Aerosp. Electron. Syst., vol. 46, no. 2, pp. 929–938, Apr. 2010.

[35] O. R. Fogle and B. D. Rigling
Micro-range/micro-Doppler decomposition of human radar signatures
IEEE Trans. Aerosp. Electron. Syst., vol. 48, no. 4, pp. 3058–3072, Oct. 2012.

[36] S. Bjorklund, H. Petersson, and G. Hendeby
Features for micro-Doppler based activity classification
IET Radar, Sonar Navig., vol. 9, no. 9, pp. 1181–1187, 2015.

[37] B. Tekeli, S. Z. Gurbuz, and M. Yuksel
Information-theoretic feature selection for human micro-Doppler signature classification
IEEE Trans. Geosci. Remote Sens., vol. 54, no. 5, pp. 2749–2762, May 2016.

[38] R. Ricci and A. Balleri
Recognition of humans based on radar micro-Doppler shape spectrum features
IET Radar, Sonar Navig., vol. 9, no. 9, pp. 1216–1223, 2015.

[39] Y. Kim and T. Moon
Human detection and activity classification based on micro-Doppler signatures using deep convolutional neural networks
IEEE Geosci. Remote Sens. Lett., vol. 13, no. 1, pp. 8–12, Jan. 2016.

[40] A. Lin and H. Ling
Three-dimensional tracking of humans using very low-complexity radar
Electron. Lett., vol. 42, no. 18, pp. 1062–1064, 2006.

[41] S. S. Ram and H. Ling
Through-wall tracking of human movers using joint Doppler and array processing
IEEE Geosci. Remote Sens. Lett., vol. 5, no. 3, pp. 537–541, Jul. 2008.

[42] Z. A. Cammenga, G. E. Smith, and C. J. Baker
High range resolution micro-Doppler analysis
Proc. SPIE, vol. 9461, 2015, Art. no. 94611G.

[43] J. Z. Kolter, S. Batra, and A. Y. Ng
Energy disaggregation via discriminative sparse coding
In *Proc. Adv. Neural Inf. Process. Syst.*, 2010, pp. 1153–1161.

[44] B. K. Natarajan
Sparse approximate solutions to linear systems
SIAM J. Comput., vol. 24, no. 2, pp. 227–234, 1995.

[45] I. W. Selesnick
Sparse signal restoration
In *Connexions*, pp. 1–13, 2006.

[46] C. M. Bishop
Pattern recognition
Mach. Learn., vol. 128, pp. 1–58, 2006.

[47] I. Ramirez, P. Sprechmann, and G. Sapiro
Classification and clustering via dictionary learning with structured incoherence and shared features
In *Proc. IEEE Conf. Comput. Vis. Pattern Recognit.*, 2010, pp. 3501–3508.

[48] M. Yang, L. Zhang, X. Feng, and D. Zhang
Fisher discrimination dictionary learning for sparse representation
In *Proc. IEEE Int. Conf. Comput. Vis.*, 2011, pp. 543–550.

[49] J. Wright, A. Y. Yang, A. Ganesh, S. S. Sastry, and Y. Ma
Robust face recognition via sparse representation
IEEE Trans. Pattern Anal. Mach. Intell., vol. 31, no. 2, pp. 210–227, Feb. 2009.

[50] F. K. Coutts, D. Gaglione, C. Clemente, G. Li, I. K. Proudler, and J. J. Soraghan
Label consistent K-SVD for sparse micro-Doppler classification
In *Proc. IEEE Int. Conf. Digit. Signal Process.*, 2015, pp. 90–94.

Shelly Vishwakarma (S'16) received the B.Tech. and M.Tech degrees in electronics and communication engineering from Guru Gobind Singh Indraprastha University, Delhi, India, in 2011 and 2013, respectively, and is currently working toward the Ph.D. degree in electrical engineering from Indraprastha Institute of Information Technology Delhi, New Delhi, India.

Her current interests include radar signal processing and machine learning.

Shobha Sundar Ram (M'11) received the Master's and Ph.D. degrees in electrical and computer engineering from the University of Texas at Austin, Austin, TX, USA, in 2006 and 2009, respectively.

She is currently an Assistant Professor at Indraprastha Institute of Information Technology Delhi, New Delhi, India. Her research interests include electromagnetic sensor conceptualization, design, and modeling.

Dr. Ram received two student paper awards at the IEEE Radar Conference in 2008 and 2009 for her work in through-wall radar tracking of humans. She is an Inspire Fellow of the Department of Science and Technology India.

Authorized licensed use limited to: Indraprastha Institute of Information Technology. Downloaded on July 21,2021 at 13:41:40 UTC from IEEE Xplore. Restrictions apply.